Supporting Information for

Modeling NH_4NO_3 over the San Joaquin Valley during the 2013 DISCOVER-AQ campaign

James T. Kelly[1], Caroline L. Parworth[2], Qi Zhang[3,4], David J. Miller[5], Kang Sun[6], Mark A. Zondlo[7], Kirk R. Baker[1], Armin Wisthaler[8], John B. Nowak[9], Sally E. Pusede[10], Ronald C. Cohen[11], Andrew J. Weinheimer[12], Andreas J. Beyersdorf[13], Gail S. Tonnesen[14], Jesse O. Bash[15], Luke C. Valin[15], James H. Crawford[9], Alan Fried[16], and James G. Walega[16]

[1]Office of Air Quality Planning and Standards, U.S. Environmental Protection Agency, RTP, NC

[2]Ames Research Center, National Aeronautics and Space Administration, Moffett Field, CA

[3]Department of Environmental Toxicology, University of California, Davis, CA

[4]Agricultural and Environmental Chemistry Graduate Group, University of California, Davis, CA

[5]Environmental Defense Fund, Boston, MA

[6]Atomic and Molecular Physics Division, Harvard-Smithsonian Center for Astrophysics, Cambridge, MA

[7]Department of Civil and Environmental Engineering, Princeton University, Princeton, NJ

[8]Institute for Ion Physics and Applied Physics, University of Innsbruck, Innsbruck, Austria

[9]Langley Research Center, National Aeronautics and Space Administration, Hampton, VA

[10]Department of Environmental Sciences, University of Virginia, Charlottesville, VA

[11]Department of Earth and Planetary Sciences, University of California at Berkeley, Berkeley, CA

[12]National Center for Atmospheric Research, Boulder, CO

[13]Department of Chemistry and Biochemistry, California State University, San Bernardino, CA

[14]Region 8, U.S. Environmental Protection Agency, Denver, CO

[15]Office of Research and Development, U.S. Environmental Protection Agency, RTP, NC

[16]Institute of Arctic and Alpine Research, University of Colorado, Boulder, CO 80309, USA

Contents of this file

Introduction

This supporting information provides additional details on measurements and model configuration, predictions, and evaluation developed according to methods described in the main article.

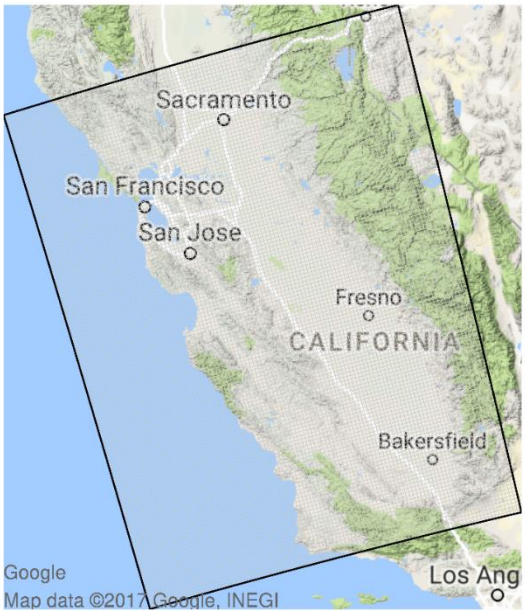

Figure S1. CMAQ modeling domain based on 4-km horizontal grid resolution.

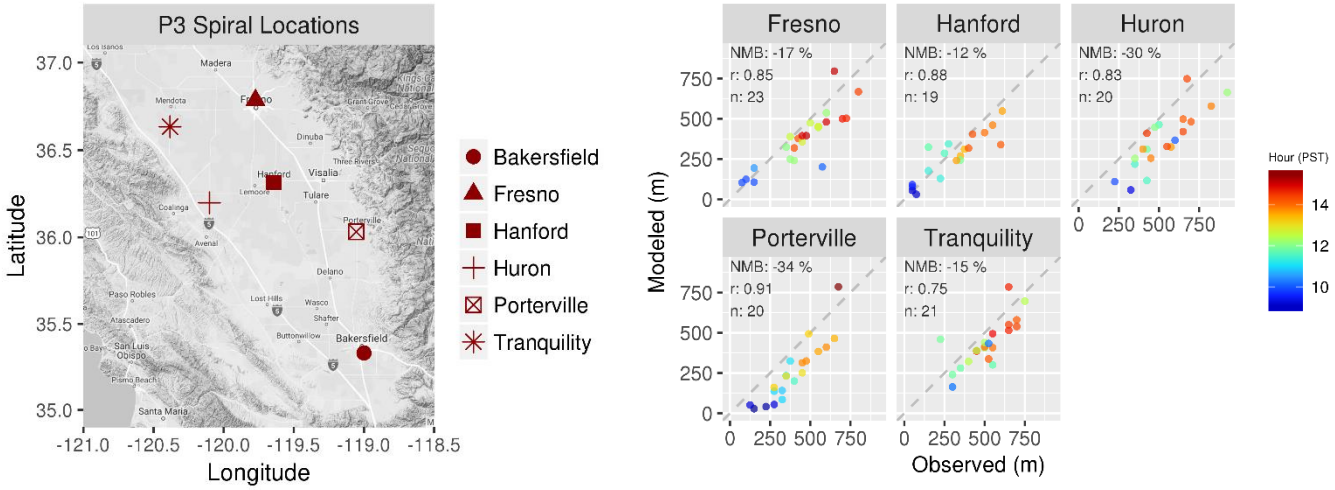

Figure S2. (a) Location of P-3B spirals and (b) comparison of modeled PBL heights and PBL heights diagnosed from P-3B measurements. NMB: normalized mean bias; r: Pearson correlation coefficient; n: number of values.

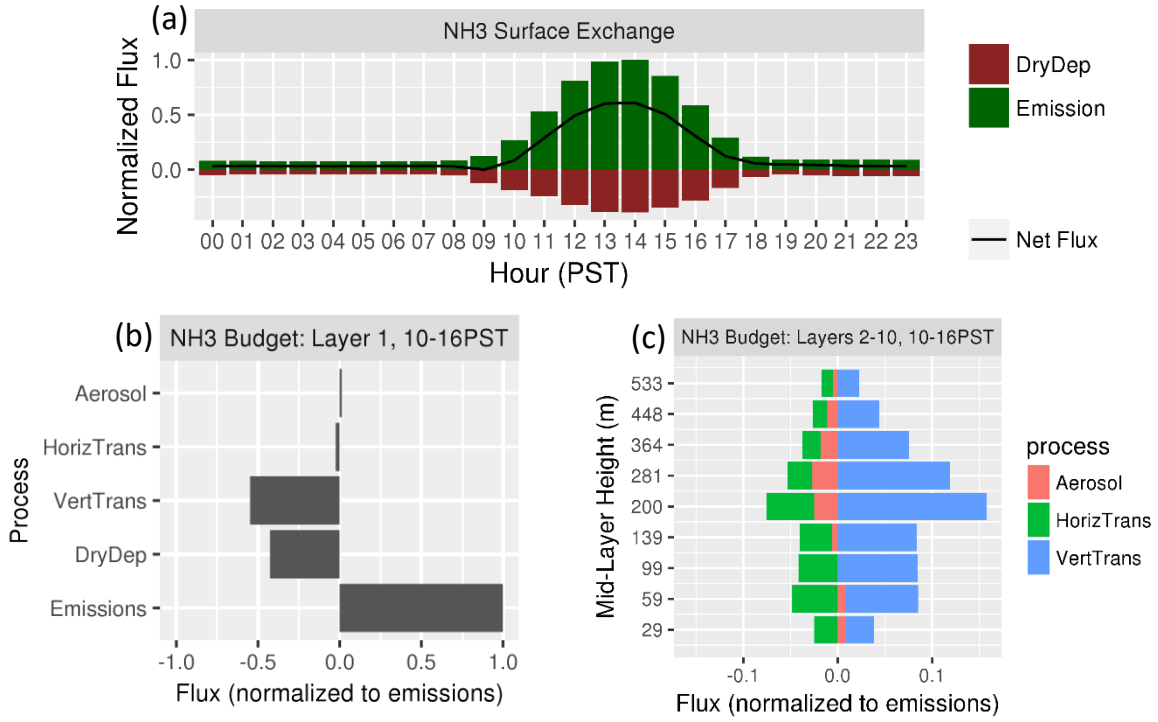

Figure S3. (a) Average hourly NH_3 emissions, deposition, and net surface exchange and (b) average NH_3 process budgets for 10-16 PST in layer 1 and (c) layers 2-10 for the region defined in Figure 1b during 15 January – 5 February 2013.

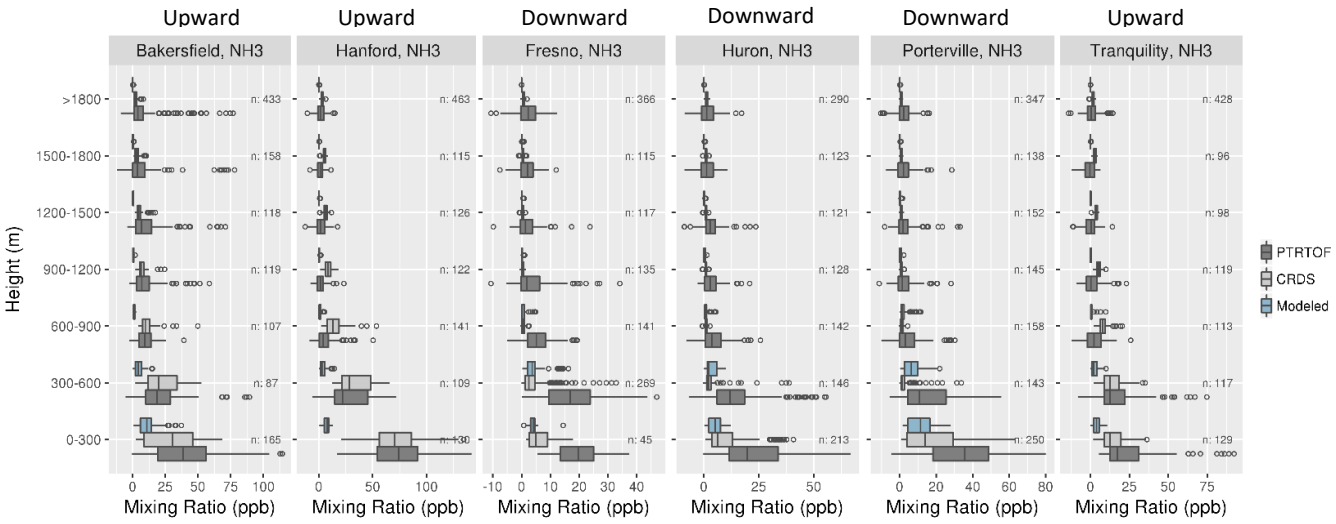

Figure S4. Comparison of modeled, CRDS, and PTR-TOF-MS NH_3 mixing ratios for P-3B spirals. The direction of the spirals is indicated to help interpret CRDS measurements that may have experienced lagging effects due to instrument response time limitations.

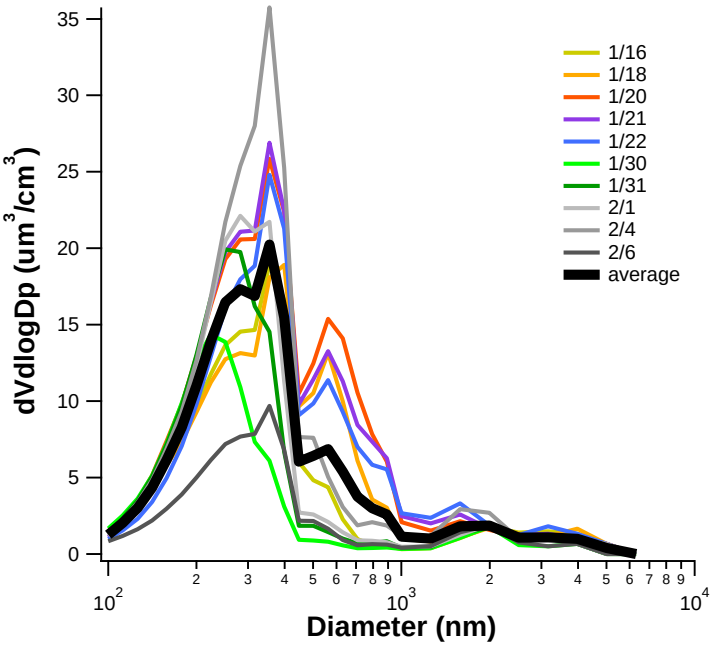

Figure S5. Particle volume size distributions during NASA-P3B aircraft flights measured by a Laser Aerosol Spectrometer based on light scattering assuming a spherical shape for samples below 1200 ft. radar altitude. On average, 95% of aerosol volume existed in the sub-1 μm size range.

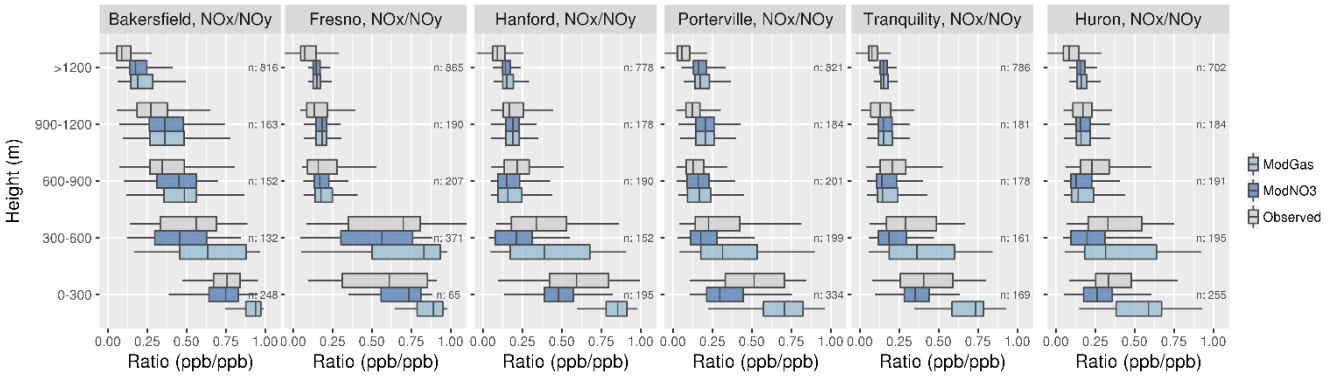

Figure S6. Comparison of measured and modeled NOx-to-NOy ratios. "ModGas" indicates ratios where modeled NOy was calculated based on summing gas-phase NOy components, and "ModNO3" indicates ratios where modeled NOy was calculated based on summing gas-phase NOy components and fine particle NO_3^-. Boxes bracket the interquartile range (IQR), lines within the boxes represent the median, and whiskers represent 1.5 times the IQR from either end of the box.

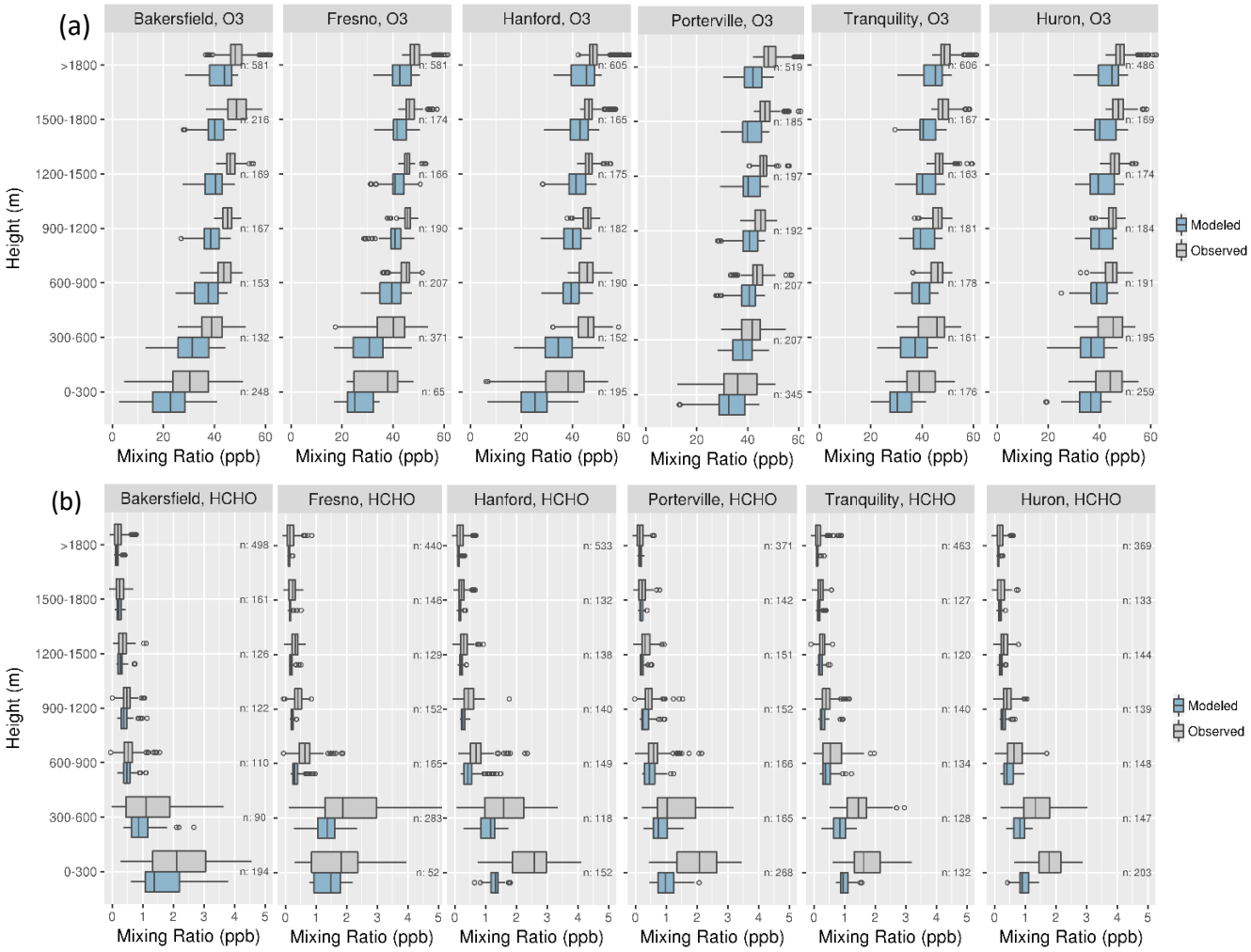

Figure S7. Comparison of modeled and measured (a) O_3 and (b) HCHO mixing ratio distributions for 300-m altitude ranges for P-3B aircraft spirals. Boxes bracket the IQR, lines within the boxes represent the median, whiskers represent 1.5 times the IQR from either end of the box, and circles represent individual values less than and greater than the range of the whiskers.

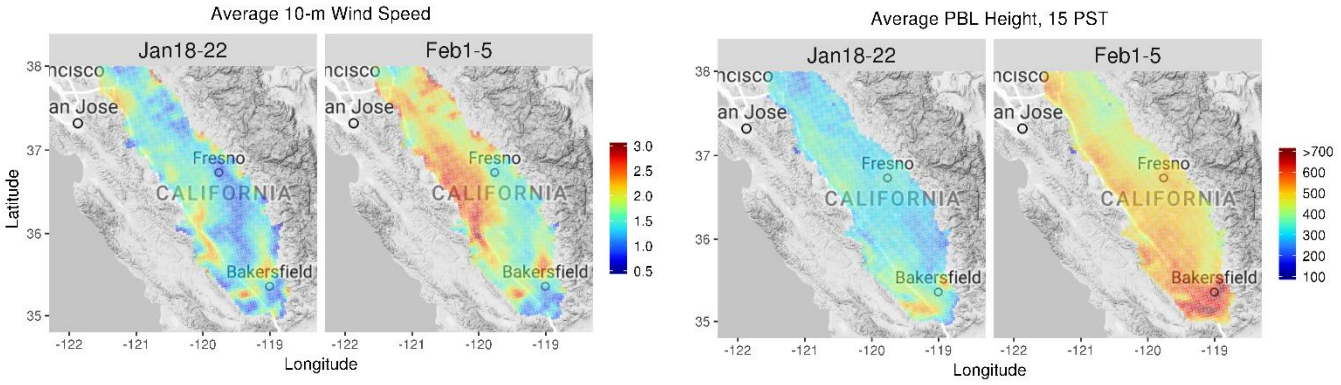

Figure S8. Average modeled 10-m wind speed and PBL height during January 18-22 and February 1-5.

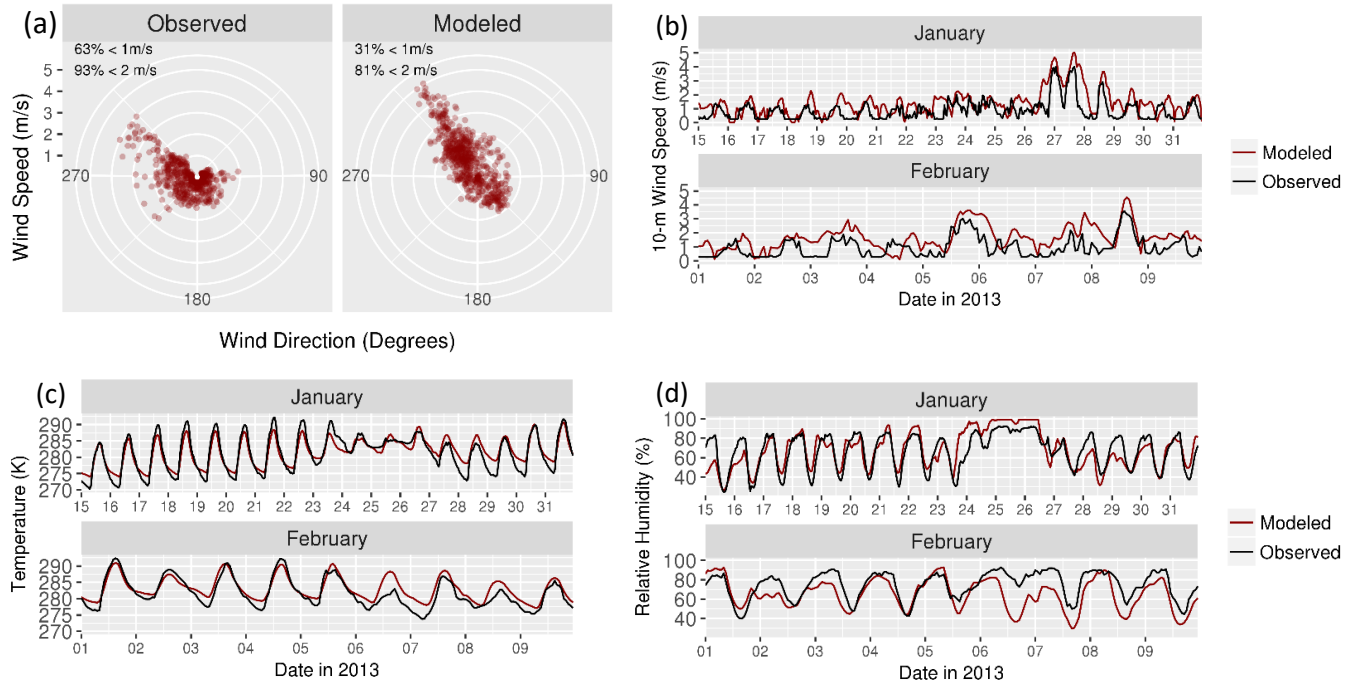

Figure S9. Fresno-Garland meteorology: (a) wind rose, (b) 10-m wind speed, (c) temperature, and (d) relative humidity. Dates are based on PST.

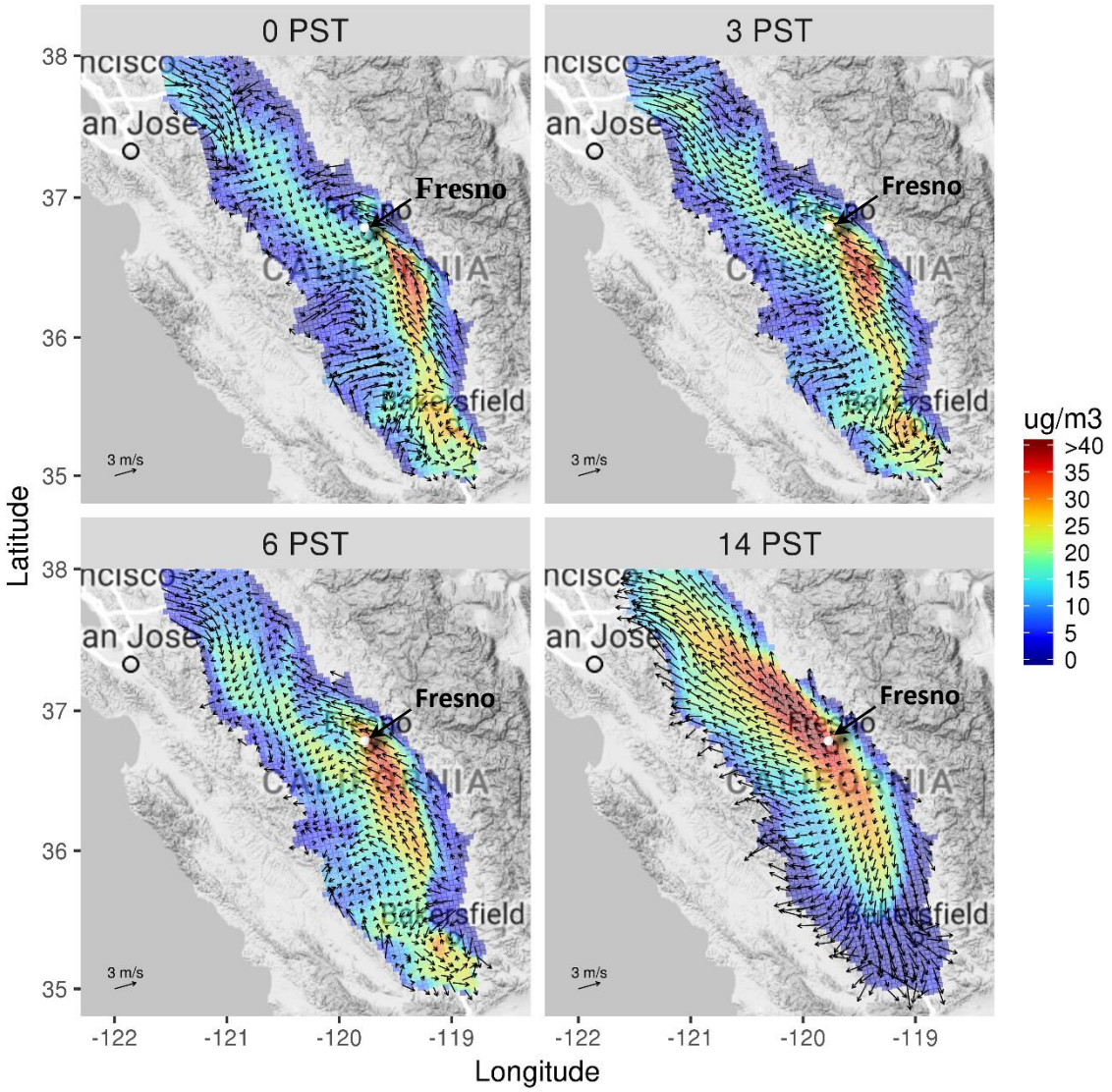

Figure S10. Modeled wind vectors and fine particle NO_3^- concentration in SJV for four hours on 22 January 2013 showing transport of NO_3^- from south of Fresno at 0 PST to the north of Fresno at 14 PST.

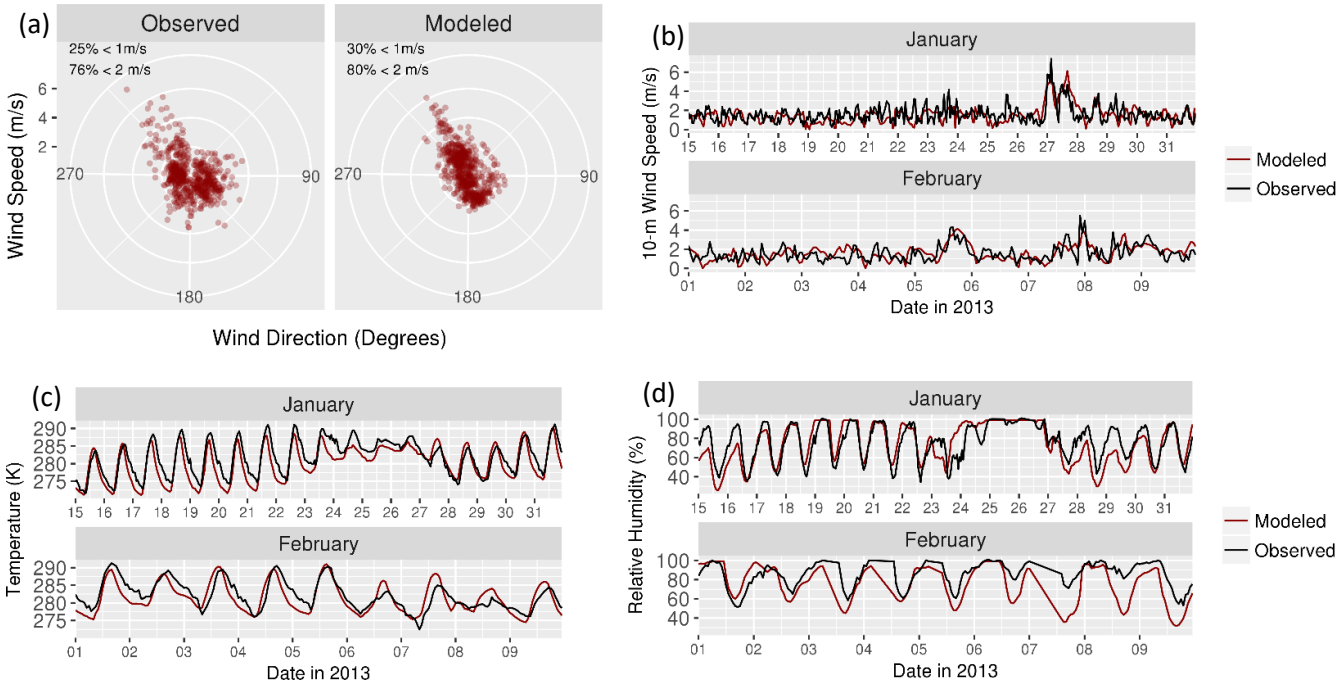

Figure S11. Visalia meteorology: (a) wind rose, (b) 10-m wind speed, (c) temperature, and (d) relative humidity.

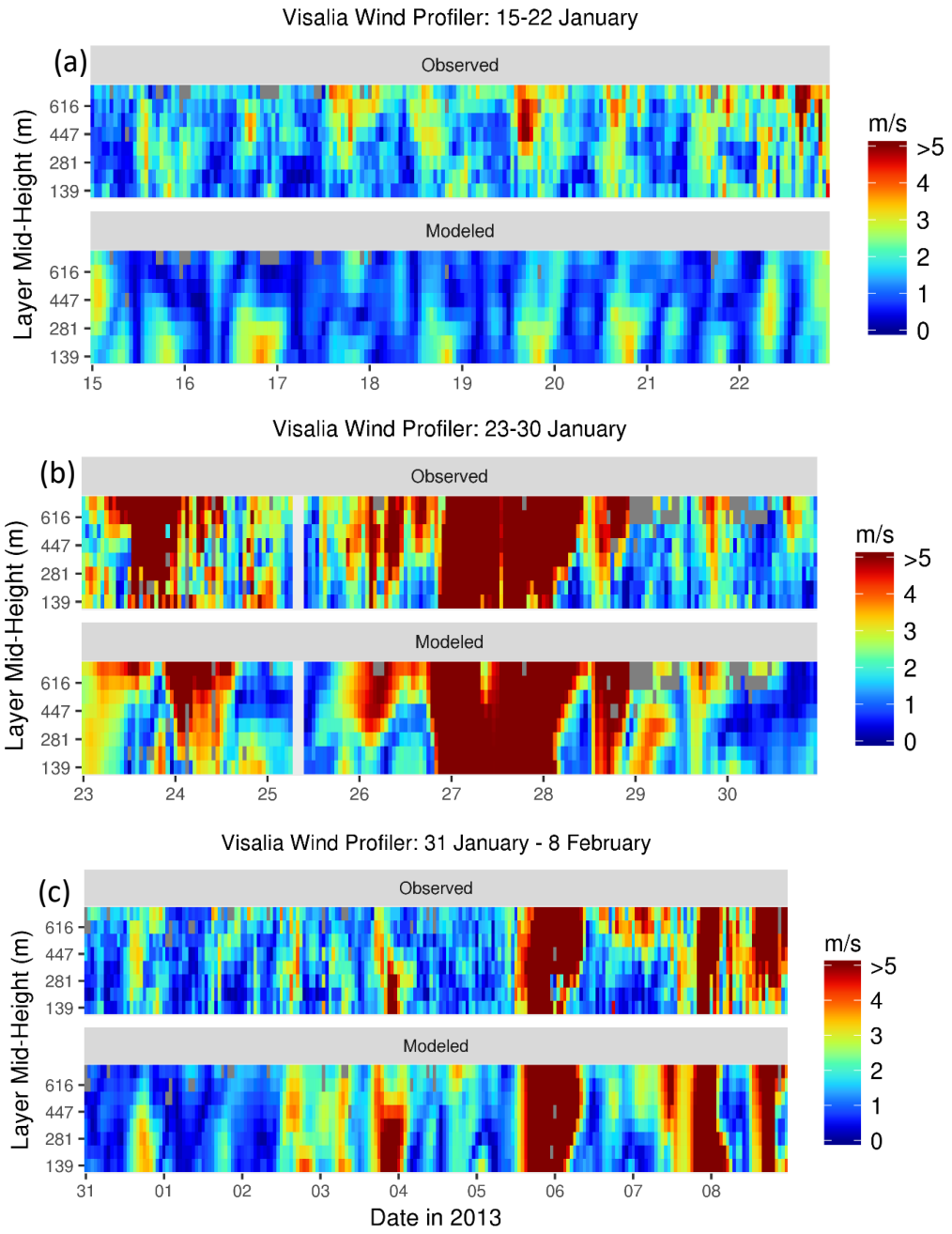

Figure S12. Observed and modeled wind speed at Visalia for (a) 15-22 January, (b) 23-30 January, and (c) 31 January – 8 February 2013. Observed values were averaged to the CMAQ grid for comparison. Values for model layers 5-12 are shown.

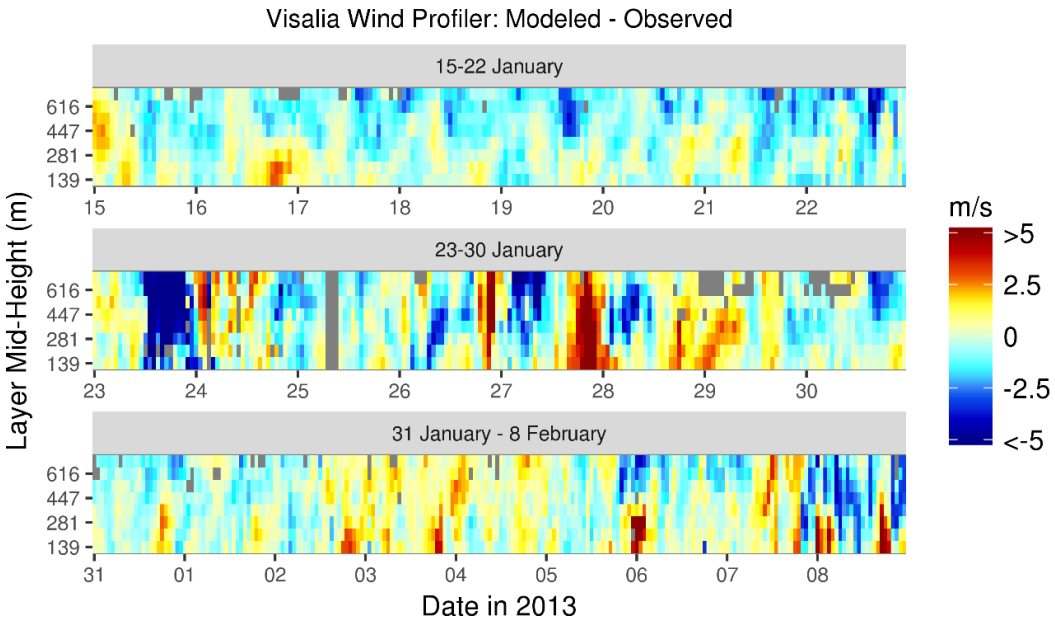

Figure S13. Difference (Modeled – Observed) in predicted and observed wind speed at Visalia for cases in Figure S12.

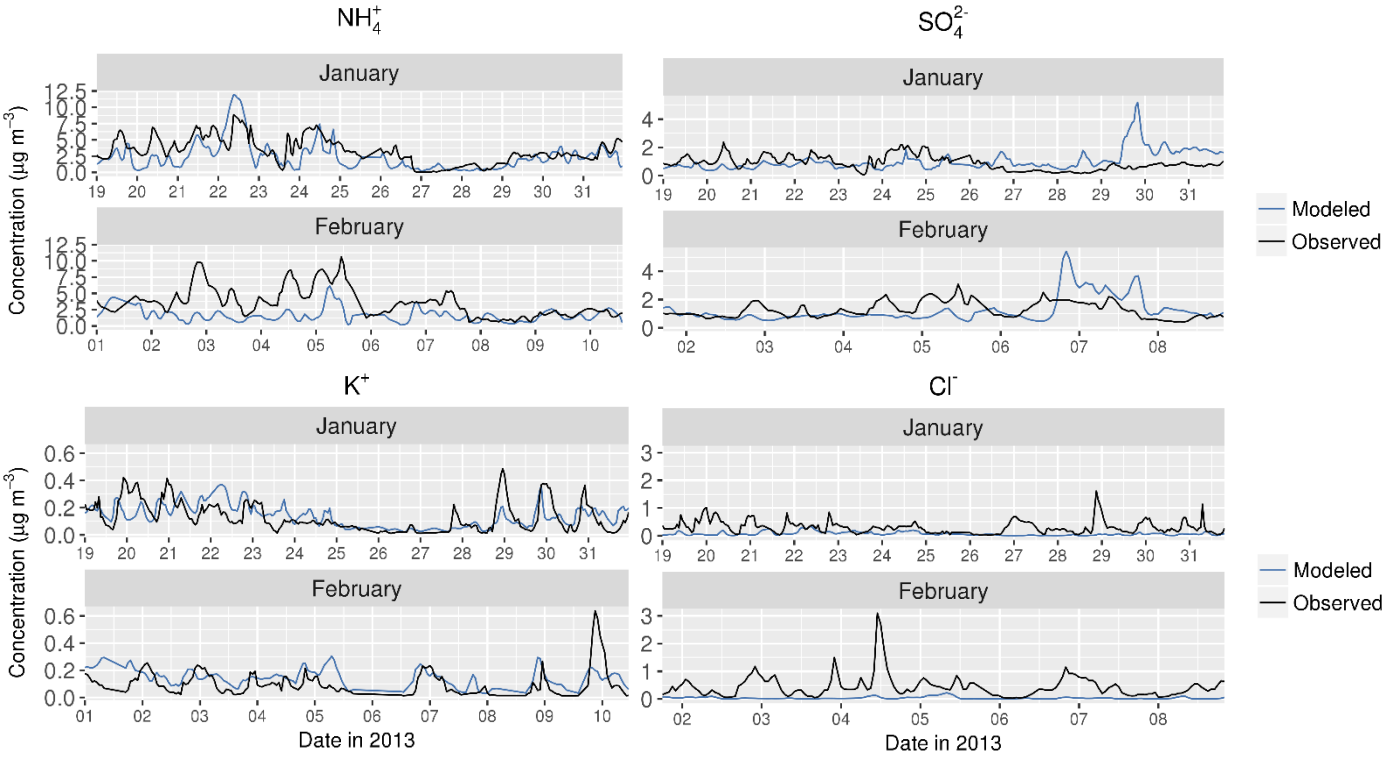

Figure S14. Comparison of model predictions of fine particle NH_4^+, SO_4^{2-}, K^+, and Cl^- with PILS-IC measurements at the Fresno-Garland ground site.

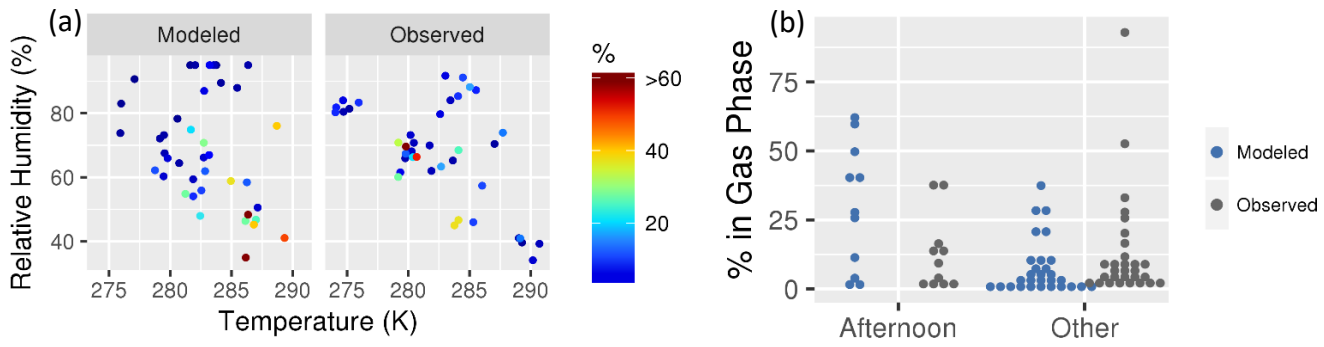

Figure S15. Percentage of TNO3 in the gas phase as a function of (a) RH and T and (b) time of day during January 19 – 31 at the Fresno ground site.

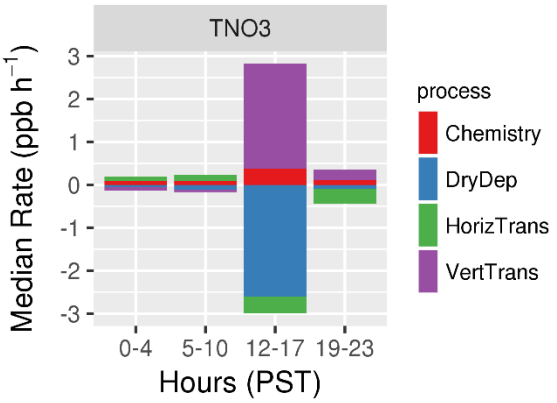

Figure S16. Median modeled process rates contributing to changes in TNO3 mixing ratios at the Fresno ground site by time of day during January 19 – 31. Chemistry: gas-phase chemistry; DryDep: dry deposition; HorizTrans: horizontal transport; VertTrans: vertical transport.

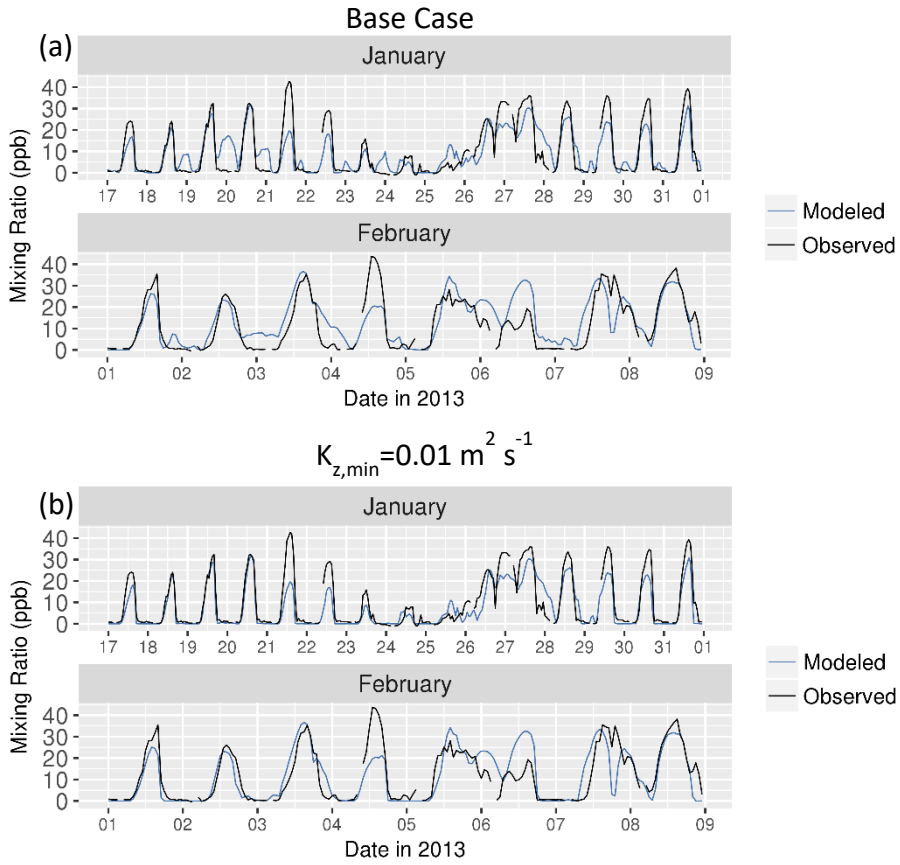

Figure S17. Comparison of model predictions and observations at the Fresno-Garland site for O_3 in the (a) base simulation and (b) the simulation with $K_{z,min}$=0.01 m^2 s^{-1}.

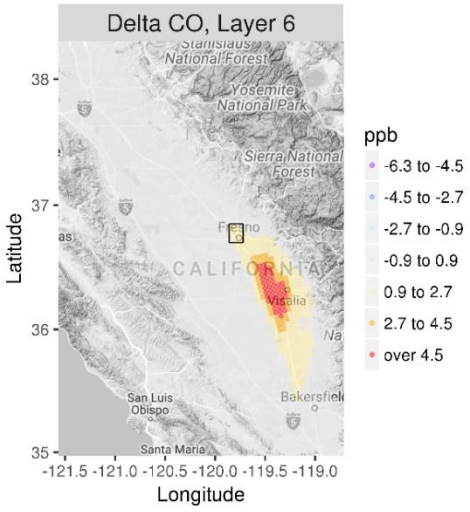

Figure S18. Average impact on CO mixing ratios in model layer 6 (160 - 240 m) during 9 PM - 4 AM PST, 17-22 January of a 15% increase in CO emissions in Fresno grid cells (i.e., grid cells in boxed region).

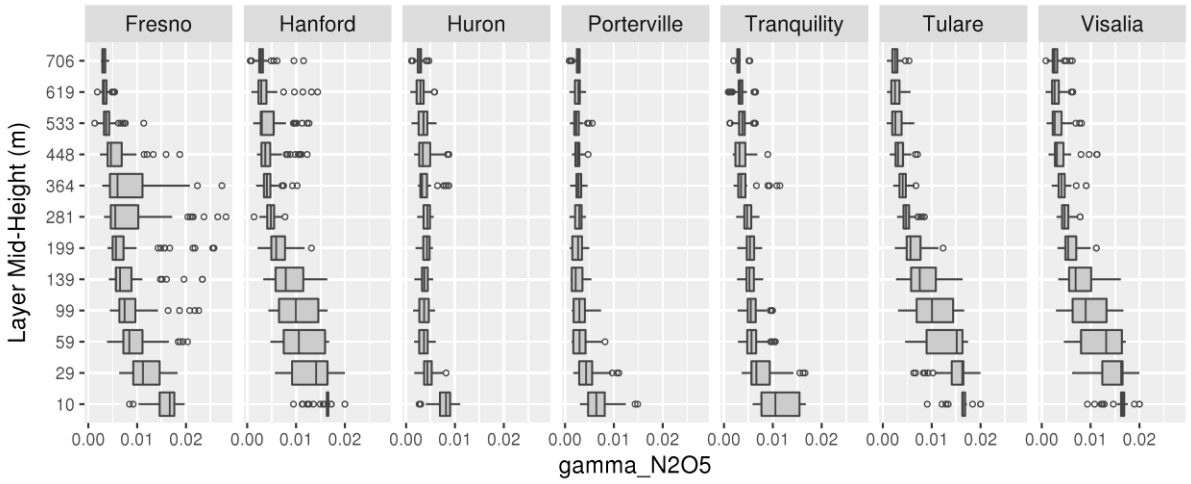

Figure S19. Model predictions of γ over P-3B spiral sites during 17-22 January 2013 for hours 20 – 6 PST.

Species	Site	N	Avg. Obs. (Range) ($\mu g\ m^{-3}$)	Avg. Mod. (Range) ($\mu g\ m^{-3}$)	NMB (%)	NME (%)	RMSE ($\mu g\ m^{-3}$)	*r*
NO_3^-	Modesto	6	7.2 (0.7-22.4)	6.8 (1.0-20.4)	-5.7	8.9	0.9	1.00
	Fresno	11	7.3 (0.9-18.6)	6.6 (1.1-24.2)	-10.5	33.8	3.0	0.89
	Visalia	6	9.4 (1.1-19.8)	7.7 (2.5-16.9)	-17.9	38.6	4.7	0.78
	Bakersfield	8	9.5 (0.0-28.1)	8.6 (2.0-18.4)	-10.0	52.2	6.6	0.85
	All	31	8.3 (0.0-28.1)	7.3 (1.0-24.2)	-11.2	36.2	4.3	0.84
SO_4^{2-}	Modesto	6	0.8 (0.1-1.7)	1.2 (0.9-1.5)	51.0	93.8	0.8	-0.71
	Fresno	11	0.7 (0.2-1.3)	1.0 (0.6-1.7)	34.8	43.5	0.4	0.43
	Visalia	6	0.9 (0.3-2.0)	0.8 (0.6-0.9)	-12.3	56.5	0.6	-0.22
	Bakersfield	8	0.9 (0.0-2.9)	1.0 (0.8-1.2)	11.4	89.5	0.9	0.02
	All	31	0.8 (0.0-2.9)	1.0 (0.6-1.7)	20.9	68.7	0.7	-0.05
Organic Carbon	Modesto	4	8.3 (1.7-16.0)	6.6 (2.6-10.4)	-21.4	29	3.9	0.79
	Fresno	9	6.7 (1.5-10.6)	6.4 (1.7-12.7)	-4.5	32.4	2.7	0.66
	Visalia	6	6.0 (1.9-9.8)	4.2 (2.2-6.4)	-30	32.3	2.2	0.98
	Bakersfield	8	4.8 (1.7-8.3)	6.0 (3.6-9.5)	25.2	35.7	1.8	0.83
	All	27	6.2 (1.5-16.0)	5.8 (1.7-12.7)	-6.6	32.4	2.6	0.69
Elemental Carbon	Modesto	4	1.8 (0.4-3.4)	1.6 (0.7-2.5)	-11.7	26.5	0.7	0.84
	Fresno	9	1.8 (0.4-3.1)	1.5 (0.4-3.3)	-16.2	35.5	0.9	0.52
	Visalia	6	1.2 (0.3-2.1)	1.0 (0.5-1.5)	-12.3	22.5	0.3	0.93
	Bakersfield	8	1.3 (0.4-2.4)	1.4 (0.7-2.5)	9.6	28.1	0.4	0.82
	All	27	1.5 (0.3-3.4)	1.4 (0.4-3.3)	-8.3	29.7	0.6	0.69

Table S1. Model performance statistics for $PM_{2.5}$ components at monitoring sites in SJV, 10 January – 9 February 2013.

Variable	Site	N	Avg. Obs. (Range)	Avg. Mod. (Range)	MB	ME	RMSE
Relative Humidity (%)	Bakersfield	510	70.6 (1-100)	63.5 (22.6-99)	-7.1	14.3	19.8
	Madera	528	77.9 (28.4-100)	74.8 (30-99)	-3.2	8.6	11.4
	Visalia	484	76.6 (34.4-101)	73.8 (25.9-99)	-2.9	10.7	13.6
	Fresno	528	67.9 (24.7-92)	67.6 (26.4-99)	-0.3	9.0	11.4
	All	2050	73.2 (1-101)	69.9 (22.6-99)	-3.3	10.6	14.4
2-m Temperature (K)	Bakersfield	522	283 (271-294)	283 (274-293)	0.2	1.9	2.2
	Hanford	527	283 (272-293)	280(271-291)	-2.8	3.1	3.7
	Porterville	526	282 (272-294)	281 (272-291)	-1.6	2.0	2.6
	Tranquility	522	282 (270-291)	281 (272-291)	-0.8	1.7	2.2
	Visalia	528	282 (272-291)	281 (271-291)	-1.8	2.4	2.9
	Fresno	528	282 (270-292)	282 (274-291)	0.3	1.7	2.1
	All	3681	282 (270-294)	281 (271-293)	-1.1	2.1	2.7
10-m Wind Speed (m/s)	Bakersfield	522	1.5 (0.3-6.1)	1.3 (0.0-4.5)	-0.2	0.7	0.9
	Hanford	527	1.4 (0.3-6.3)	1.7 (0.0-6.2)	0.3	0.7	0.9
	Porterville	526	1.7 (0.3-4.7)	1.7 (0.0-4.0)	-0.1	0.8	1.0
	Tranquility	522	2.5 (0.3-8.8)	2.3 (0.0-7.9)	-0.3	0.8	1.0
	Visalia	528	1.6 (0.3-7.4)	1.5 (0.0-6.1)	-0.1	0.7	0.9
	Fresno	528	0.9 (0.3-4.0)	1.4 (0.0-5.0)	0.5	0.7	0.9
	All	3681	1.6 (0.3-8.8)	1.7 (0.0-7.9)	0.0	0.7	1.0

Table S2. Model performance statistics for meteorological variables at sites in SJV, 15 January – 5 February 2013.

Period	Layer Half Height (m)	N	Obs Mean (Range) (m/s)	Mod Mean (Range) (m/s)	NMB (%)	MB (m/s)	RMSE (m/s)	*r*
15 Jan -22 Jan	139	192	1.57 (0.25-4.50)	1.46 (0.11-3.74)	-7.4	-0.1	1.0	0.27
	200	192	1.42 (0.00-3.60)	1.53 (0.16-3.52)	7.3	0.1	0.9	0.32
	281	192	1.59 (0.05-3.55)	1.51 (0.05-3.13)	-4.9	-0.1	0.9	0.28
	364	192	1.70 (0.23-4.17)	1.35 (0.09-3.18)	-20.3	-0.3	1.0	0.18
	447	191	1.86 (0.30-5.30)	1.18 (0.01-3.28)	-36.5	-0.7	1.2	0.24
	532	192	1.94 (0.40-6.05)	1.11 (0.16-3.25)	-42.5	-0.8	1.3	0.26
	616	188	2.15 (0.47-6.20)	1.09 (0.09-2.96)	-49.2	-1.1	1.5	0.28
	702	175	2.34 (0.20-5.90)	1.18 (0.11-3.01)	-49.6	-1.2	1.5	0.25
23 Jan - 30 Jan	139	188	2.72 (0.10-11.40)	3.01 (0.14-10.51)	10.5	0.3	1.8	0.71
	200	182	2.95 (0.10-18.30)	3.14 (0.18-12.21)	6.4	0.2	2.4	0.66
	281	188	3.44 (0.20-14.30)	3.25 (0.27-13.68)	-5.3	-0.2	2.3	0.72
	364	186	3.75 (0.30-16.63)	3.45 (0.12-14.71)	-7.9	-0.3	2.6	0.71
	447	184	4.16 (0.50-17.45)	3.60 (0.12-15.32)	-13.5	-0.6	2.8	0.71
	532	186	4.41 (0.10-17.65)	3.86 (0.14-15.04)	-12.3	-0.5	2.7	0.73
	616	167	5.25 (0.30-20.10)	4.40 (0.15-14.06)	-16.1	-0.8	3.3	0.62
	702	168	5.29 (0.65-19.9)	4.65 (0.09-13.27)	-12.0	-0.6	2.9	0.67
31 Jan - 8 Feb	139	216	2.00 (0.30-10.65)	2.50 (0.19-10.25)	25.0	0.5	1.5	0.77
	200	215	2.01 (0.10-11.80)	2.49 (0.13-11.26)	23.5	0.5	1.7	0.77
	281	216	2.33 (0.25-12.60)	2.60 (0.08-13.78)	11.7	0.3	1.9	0.73
	364	216	2.68 (0.13-13.75)	2.73 (0.05-15.4)	1.7	0.0	1.2	0.91
	447	214	2.85 (0.10-14.65)	2.70 (0.04-13.75)	-5.0	-0.1	1.2	0.90
	532	214	2.88 (0.20-14.40)	2.74 (0.09-11.91)	-5.0	-0.1	1.3	0.89
	616	207	2.97 (0.20-13.10)	2.70 (0.27-10.01)	-9.1	-0.3	1.4	0.86
	702	204	2.98 (0.40-12.30)	2.65 (0.25-8.32)	-11.0	-0.3	1.5	0.83

Table S3. Comparison statistics for modeled and observed wind speeds at Visalia shown in Figure S12 and S13.

	R1 (μmol m^{-2} day^{-1})	R2 (μmol m^{-2} day^{-1})	Total (μmol m^{-2} day^{-1})	% R1	% R2	% Change from Total Production in Base
Base	79,605	94,469	174,074	46	54	0
40% NOx Emission Reduction	50,087	52,419	102,506	49	51	-41
0.5 γ_{N2O5}	83,495	72,184	155,679	54	46	-11
1.5 γ_{N2O5}	77,463	106,327	183,790	42	58	6
Y=0 (no het. $ClNO_2$)	79,028	94,037	173,065	46	54	-1

Table S4. Summary of HNO_3 production during 17-22 January 2013 for base and sensitivity simulations for model layers 1-20 over SJV.